

Actively coupled optical waveguides

N. V. Alexeeva^{1,2}, I. V. Barashenkov^{1,2}, K. Rayanov¹ and S. Flach¹

*New Zealand Institute for Advanced Study, Centre for Theoretical Chemistry and Physics,
Massey University, Auckland 0745, New Zealand*

² *Department of Mathematics and Centre for Theoretical and Mathematical Physics,
University of Cape Town, Rondebosch 7701, South Africa*

We consider light propagation through a pair of nonlinear optical waveguides with absorption, placed in a medium with power gain. The active medium boosts the in-phase component of the overlapping evanescent fields of the guides, while the nonlinearity of the guides couples it to the damped out-of-phase component creating a feedback loop. As a result, the structure exhibits stable stationary and oscillatory regimes in a wide range of gain-loss ratios. We show that the pair of actively-coupled (\mathcal{AC}) waveguides can act as a stationary or integrate-and-fire comparator sensitive to tiny differences in their input powers.

Introduction.— Nonlinear directional couplers are important for various applications in integrated optics, such as power-sensitive switches and polarization beam splitters. The twin core coupler is based on the coherent light exchange between two optical waveguides placed in close proximity. For low input intensities, the full power oscillates periodically between the two waveguides; for higher input levels, the total power is selftrapped mainly in one of the two channels [1].

The performance of the device can be improved — the switching power reduced while the length shortened — by utilizing material losses. The effect of absorption which is usually regarded as an unavoidable hinder, is therefore turned into advantage here. The dissipation is balanced by introducing gain into one of the waveguides [2]. Thus, a nonlinear coupler composed of one core with a certain amount of gain and another one with an equal amount of loss switches the entire power to one waveguide [3]. Recently this type of a coupler has attracted a lot of attention as an experimental realisation of a \mathcal{PT} -symmetric system [4]. It is worth noting here that the operation of the \mathcal{PT} -symmetric coupler requires the fine-tuning of gain and loss, to secure their exact compensation. We also note that the power switching is accompanied by the unbounded power growth in one of the arms of the device — the growth not saturable by nonlinearity [4].

In this Letter, we propose a conceptually new configuration of gain and loss in the directional coupler. The arrangement consists of two lossy waveguides placed in an active medium. Instead of providing power gain in the core of a waveguide, the structure boosts the evanescent fields which couple the two channels due to their close proximity. Choosing the symmetric gain configuration, the energy is pumped into the in-phase linear mode of the two-waveguide system while the anti-phase normal mode remains lossy.

The operation of the outlined device (the actively coupled pair of waveguides, or simply “ \mathcal{AC} -coupler”) is conditional on the presence of nonlinearity. As the symmetric mode starts to grow, it activates the nonlinear response in each waveguide; the nonlinearity couples the

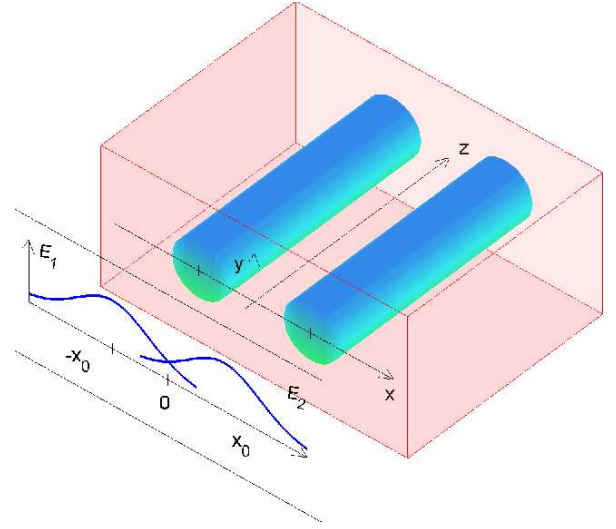


FIG. 1. (Color online) The \mathcal{AC} coupler: two parallel lossy waveguides coupled via an active medium. The stand-alone vertical plane shows the eigenfunctions $E_1(x, 0)$ and $E_2(x, 0)$.

symmetric to antisymmetric mode which drains the energy out of the system securing the overall power balance. The concept admits generalisations to networks of waveguides, with various coupling geometries. It can also find applications outside the realm of optics, e.g. in the context of structured metamaterials [5] and interacting exciton-polariton condensates [6].

The \mathcal{AC} -coupler is structurally stable — in order to ensure the gain-loss balance, one need not strive to secure the perfect equality of gain and loss. Instead, the loss compensation is achieved in a finite band of gain coefficients. Unlike the usual nonlinear optical coupler, and unlike the \mathcal{PT} -coupler, the observable regimes in the new configuration are determined by the system parameter values rather than initial conditions. Furthermore, the system does not exhibit any uncontrollable growth of optical modes.

Model. — In a single-mode optical waveguide, the opti-

cal field is described by a complex amplitude $\Psi(x, y, z) = E(x, y)\psi(z)$, where (x, y) is the plane transversal to the waveguide axis z . The eigenfunction $E(x, y)$ decays away from the waveguide core and can be chosen to be real and everywhere positive, with the norm $\int E^2 dx dy = 1$.

We consider two parallel identical waveguides. Denoting x the coordinate in the direction connecting their centres, we choose the origin halfway between them. The individual eigenfunctions E_1 and E_2 are then centred at $x = -x_0$ and $x = x_0$, respectively, and satisfy $E_1(x, y) = E_2(-x, y)$. The waveguides are embedded in the active medium (Fig.1) and gain power through the response of the medium to the evanescent part of their fields, Ψ_1 and Ψ_2 .

The integral gain of the amplitude $\psi_n(z)$ over the entire active region is $\int \alpha E_n(x, y) \Psi dx dy$, where $\Psi(x, y, z)$ is the sum of the two evanescent fields: $\Psi = \Psi_1(x, y, z) + \Psi_2(x, y, z)$. The coefficient $\alpha(x, y) \geq 0$ characterises the active properties of the medium. The integral gain in each waveguide is then $a_{n1}\psi_1 + a_{n2}\psi_2$, where

$$a_{nm} = \int \alpha(x, y) E_n(x, y) E_m(x, y) dx dy, \quad n, m = 1, 2.$$

With the gain added, the amplitudes ψ_1 and ψ_2 satisfy

$$\frac{d\psi_1}{dz} + \Gamma\psi_1 = i\mathcal{T}\psi_2 + i\beta|\psi_1|^2\psi_1 + \sum a_{1n}\psi_n, \quad (1a)$$

$$\frac{d\psi_2}{dz} + \Gamma\psi_2 = i\mathcal{T}\psi_1 + i\beta|\psi_2|^2\psi_2 + \sum a_{2n}\psi_n. \quad (1b)$$

Here Γ is the loss rate, β the nonlinearity strength, and \mathcal{T} quantifies light tunneling between the guides [7]. In what follows, we assume the focussing nonlinearity, $\beta > 0$. We scale $\psi_{1,2}$ so that $\beta = 1$ and normalise \mathcal{T} to 1.

We note that $a_{12} = a_{21}$. Assuming symmetric density distributions $\alpha(x, y) = \alpha(-x, y)$ we also have $a_{11} = a_{22}$. From $E_{1,2}(x, y) > 0$ it follows that $a_{mn} > 0$. Using the Schwartz inequality, one readily checks that a_{11} is always greater than a_{12} . All coefficients become equal only when the active region is very thin: $\alpha(x, y) = \alpha_0(y)\delta(x)$. In this case we have $a_{11} = a_{12} = \int \alpha_0(y) E_1^2(0, y) dy$.

In the general situation of symmetrically distributed gain, we introduce the net loss rate $\gamma = \Gamma - a_{11}$ and the active coupling (\mathcal{AC}) coefficient $a \equiv a_{12}$ to obtain

$$\frac{d\psi_1}{dz} + \gamma\psi_1 = i\psi_2 + i|\psi_1|^2\psi_1 + a\psi_2, \quad (2a)$$

$$\frac{d\psi_2}{dz} + \gamma\psi_2 = i\psi_1 + i|\psi_2|^2\psi_2 + a\psi_1. \quad (2b)$$

In this Letter, we consider the regime where $\gamma > 0$.

Dynamics of coupled beams.— When the net loss exceeds the \mathcal{AC} gain ($\gamma > a$), all solutions of (2) decay to zero:

$$\frac{dP}{dz} \leq 2(a - \gamma)P. \quad (3)$$

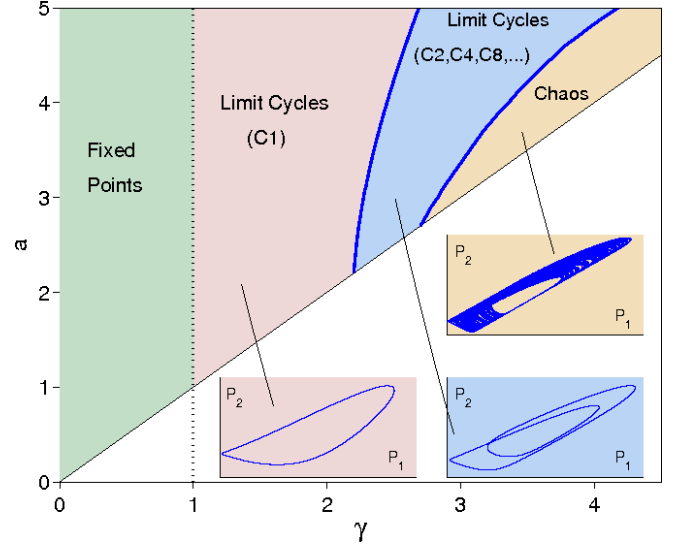


FIG. 2. (Color online) The chart of attractors on the (γ, a) plane. In the empty area below the $\gamma = a$ line, all initial conditions decay to zero as $t \rightarrow \infty$. In the green strip, the attractors are the fixed points F^\pm . Pink marks the region where all trajectories wind onto one of the two limit cycles C^\pm , with one simple oscillation per period (hence “C1”). In the blue domain the attracting cycles have 2^n (i.e. 2, 4, 8, ...) simple oscillations per period. The ochre colours the area where the attractors are predominantly chaotic; these consist of repeated oscillations with randomly selected amplitudes. Three insets are phase portraits on the (P_1, P_2) plane: a cycle with one and two oscillations per period, and a chaotic attractor.

Here $P = |\psi_1|^2 + |\psi_2|^2$ is the total power of light in the coupler. Thus in the region below the $\gamma = a$ line in Fig.2, the origin $\psi_1 = \psi_2 = 0$ is a globally stable fixed point.

Introducing the symmetric and antisymmetric normal modes $u = \psi_1 + \psi_2$ and $v = \psi_1 - \psi_2$ diagonalises the linear part of (2) — but couples the nonlinear terms:

$$\frac{du}{dz} + (\gamma - a - i)u = \frac{i}{4}[(|u|^2 + 2|v|^2)u + v^2u^*], \quad (4a)$$

$$\frac{dv}{dz} + (\gamma + a + i)v = \frac{i}{4}[(2|u|^2 + |v|^2)v + u^2v^*]. \quad (4b)$$

According to (4a), making a greater than γ turns the origin into an unstable fixed point. In the $a > \gamma$ regime with $v(0) = 0$, the symmetric mode grows without bound. However the blow-up of the u -mode can be arrested by its nonlinear coupling to the antisymmetric mode.

Decomposing the complex amplitudes as $\psi_1 = \sqrt{P_1}e^{i\phi}$ and $\psi_2 = \sqrt{P_2}e^{i(\phi+\theta)}$, we observe that the common part of the phases of the two beams is expressible through the powers they carry and their phase difference:

$$\phi(z) = \int_0^z \left[P_1 + \sqrt{\frac{P_2}{P_1}}(\cos \theta + a \sin \theta) \right] dz + \phi(0).$$

Therefore out of four real variables in the system (2) only three represent independent degrees of freedom.

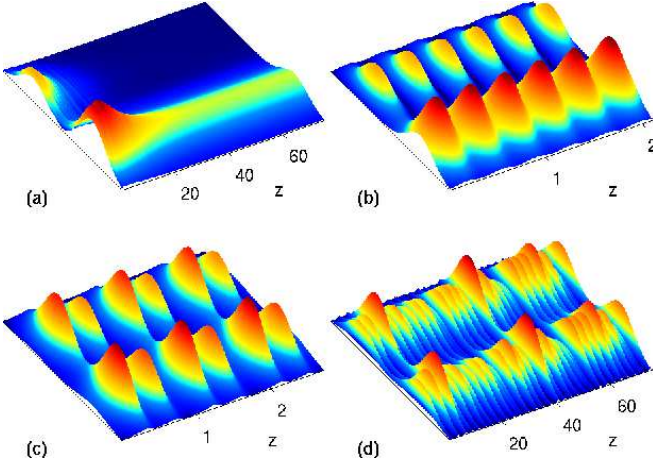


FIG. 3. (Color online) Characteristic regimes of the AC coupler. Shown is $|E_1(x,0)\psi_1(z) + E_2(x,0)\psi_2(z)|^2$, with the eigenfunctions exemplified by $E_{1,2}(x,0) = \frac{1}{\sqrt{2\pi\nu}} \exp\left(\frac{-(x \pm x_0)^2}{2\nu^2}\right)$, $\nu = \frac{3}{5}x_0$. (a) The stationary regime F^+ evolving out of the initial condition with $P_1 = 30$, $P_2 = 33$, $\theta = 0$. Here $a = 1$, $\gamma = 0.1$. (b) The limit cycle C^+ ($a = 9$, $\gamma = 1.5$). (c) The limit cycle with two oscillations per period ($a = 9$, $\gamma = 4.2$). (d) The chaotic attractor ($a = 9$, $\gamma = 7.6$).

This fact is made obvious by transforming the system to an explicitly three-dimensional form:

$$\dot{X} = -\gamma X - Y, \quad (5a)$$

$$\dot{Y} = -\gamma Y + X - XZ, \quad (5b)$$

$$\dot{Z} = -\gamma Z + aZ + XY. \quad (5c)$$

Here $X = \frac{1}{2}(|\psi_1|^2 - |\psi_2|^2)$ measures the power imbalance between the two waveguides; $Y = \frac{i}{2}(\psi_1\psi_2^* - \psi_1^*\psi_2)$ characterizes the energy flux from the first to the second channel, and $2aZ$ — where $Z = \frac{1}{2}(\psi_1\psi_2^* + \psi_2\psi_1^*)$ — is the total gain in the system. The Stokes variables X, Y , and Z are three components of the vector \mathbf{r} , with $r = \sqrt{\mathbf{r}^2} = P/2$. The overdot indicates differentiation with respect to the fictitious time variable, $t = 2z$, which we introduce for convenience of analysis.

The beam powers $P_{1,2}$ and the phase difference θ can be easily reconstructed from the Stokes variables: $P_{1,2} = r \pm X$ and $\tan \theta = Y/Z$. We also note a similarity between equations (5) and the Lorentz system [8].

Symmetry-broken fixed points. — Like the Lorentz system, Eqs.(5) are symmetric under the reflection of X and Y . As the AC coefficient is increased beyond $a = \gamma$ in the weakly-dissipative regime ($\gamma < 1$), the fixed point at the origin suffers a symmetry-breaking (pitchfork) bifurcation. Two stable fixed points F^+ and F^- are born, supercritically. These points share the values of r and Z ,

$$r = (\gamma^2 + 1)\frac{a}{\gamma}, \quad Z = \frac{\gamma}{a}r, \quad (6)$$

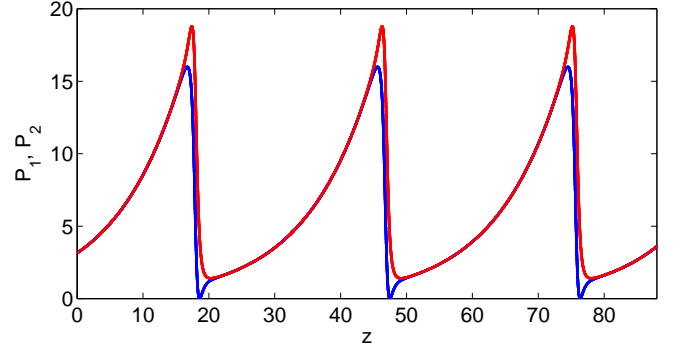


FIG. 4. (Color online) The integrate-and-fire limit cycle arising for γ close to a . (In this plot, $\gamma = 1.9$ and $a = 2$.) The red and blue line show P_2 and P_1 , respectively.

but have opposite X and Y :

$$X = -\frac{\sigma}{a}r, \quad Y = \sigma\frac{\gamma}{a}r. \quad (7)$$

The point F^+ has $\sigma > 0$ and F^- has $\sigma < 0$, where $\sigma^2 = (a^2 - \gamma^2)/(\gamma^2 + 1)$. The two points are therefore mirror images of each other.

Either of the two fixed points represents a pair of light beams with constant, z -independent, power in each channel. The point F^+ corresponds to a greater power in the second channel ($P_1/P_2 \approx \gamma^2/2$ for small γ), while its mirror reflection F^- has the inverse power ratio. The phases ϕ_1 and ϕ_2 pertaining to the points F^\pm are linear functions of z , with the phase difference θ remaining constant.

Fig.3(a) depicts the evolution of the input with a small power imbalance. We observe that taking $P_2(0)$ only slightly greater than $P_1(0)$ is sufficient to select the stationary regime (F^+) with $P_2 \gg P_1$.

Periodic and chaotic regimes. — Linearizing Eqs.(5) about either of the fixed points F^\pm yields the Jacobian matrix with one real negative and two complex-conjugate eigenvalues λ . Assume the active coupling is fixed above the threshold value $a = 1$ and the net loss γ is varied. As γ is increased through $\gamma_c = 1$, the complex eigenvalues cross from $\text{Re } \lambda < 0$ to $\text{Re } \lambda > 0$. This is the signature of the Hopf bifurcation where both F^+ and F^- lose their stability while two stable limit cycles of small radius are born — one around each fixed point.

The limit cycles describe periodic variation of the powers $P_{1,2}$ carried by the two waveguides [Fig.3(b)]. We denote C^+ the cycle born around the point F^+ and C^- the cycle bifurcating from F^- .

Like their parent fixed points F^\pm , the limit cycles C^\pm are symmetry broken. The cycle C^+ has the second waveguide carrying higher power than the first one, while its mirror-reflected counterpart C^- has $P_1(z) > P_2(z)$ for all z . When $\gamma = \gamma_c$, the frequency of each cycle is given by $\omega = \text{Im } \lambda = \sqrt{a^2 - 1}$. As γ is increased beyond γ_c , the radius grows and the frequency changes.

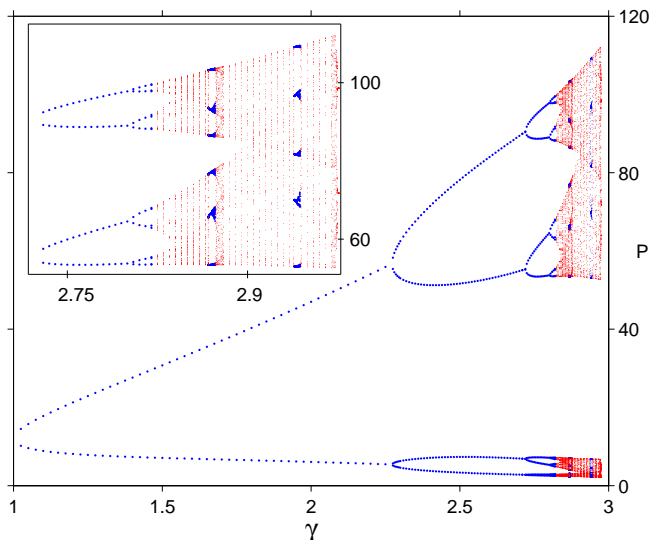


FIG. 5. (Color online) The period-doubling transition to chaos for $a = 3$. The local minima and maxima of the function $P(z)$ are plotted against the corresponding value of the loss coefficient. The inset shows a fine structure of the chaotic region. Periodic attractors are marked by blue; chaotic by red.

The limit cycles with γ near a display an integrate-and-fire switch dynamics (Fig.4). Namely, the powers in the two waveguides grow slowly and synchronously, with one of these (say, P_1) remaining only slightly smaller than the other power (P_2). This is followed by a quick discharge, where the first waveguide loses practically all its power ($P_1 = 0$) while P_2 remains nonzero.

As the loss γ is increased with the value of active coupling fixed above $a = 2.2$, the limit cycle suffers a period doubling. The emerging periodic attractor with two oscillations per period is shown in Fig.3(c) and the middle inset in Fig.2. Increasing γ further, the limit cycle undergoes a cascade of higher period-doubling bifurcations (Fig.5). This culminates in the emergence of chaotic attractors [Fig.3(d) and the top inset in Fig.2]. The set of parameter values corresponding to periodic attractors with 2^n oscillations per period ($n = 1, 2, \dots$), is marked blue in Fig.2, and the “chaotic domain” is ochre-colored.

Conclusions.— We conclude our study of the \mathcal{AC} coupler by crystallising its key difference from the \mathcal{PT} symmetric device. While the latter balances gain in one waveguide with loss in the other, the former treats its two channels equally. It is the symmetric and antisymmetric normal modes (rather than the two guides themselves) that serve as the gain and loss agents in the \mathcal{AC} configuration.

An important advantage of the \mathcal{AC} coupler is its structural stability. For the given loss rate, the system supports stationary and periodic light beams in a wide range

of gain coefficients rather than for a particular value of a . This is a fundamental distinction from the \mathcal{PT} -symmetric coupler where one has to tune the gain to match the loss exactly [4].

The new properties exhibited by the device can be utilised in a variety of applications. One possible setting is an optical analog of the voltage comparator which swings its output to one of two values depending on the relation between its two input voltages. The \mathcal{AC} coupler can operate either in the stationary regime, where the two output values are given by the fixed points of the system (5), or as an integrate-and-fire switch (Fig.4), where one of the waveguides is left powerless periodically. The period of this oscillator can be tuned simply by varying the distance between the waveguides. Unlike the \mathcal{PT} -symmetric coupler, no input can trigger an uncontrollable growth of optical modes in the \mathcal{AC} -switch.

Acknowledgments.— N.A. and I.B.’s sabbatical leave in Auckland was funded via visiting fellowships of the New Zealand Institute for Advanced Study. The project was also supported by the NRF of South Africa (Grants UID 85751 and 78950) and the Vera Davie study and research bursary from UCT.

REFERENCES

- [1] S M Jensen, Journ. Quantum Electronics **18** 1580 (1982); A W Snyder and Y Chen, Opt. Lett. **14** 517 (1989)
- [2] M. Premaratne and G. P. Agrawal, *Light Propagation in Gain Media*. Cambridge University Press, Cambridge (2011)
- [3] Y. Chen, A. W. Snyder, and D. N. Payne, IEEE Journ. Quant. Electronics **28** 239 (1992)
- [4] H. Ramezani, T. Kottos, R. El-Ganainy, D.H. Christodoulides, Phys. Rev. A **82** 043803 (2010); A.A. Sukhorukov, Z.Y. Xu, Yu.S. Kivshar, Phys. Rev. A **82** 043818 (2010); C. E. Rüter, K. G. Makris, R. El-Ganainy, D.N. Christodoulides, M. Segev, and D. Kip, Nat. Phys. **6** 192 (2010); T. Kottos, *ibid.* 166; Z. Lin, H. Ramezani, T. Eichelkraut, T. Kottos, H. Cao, and D.N. Christodoulides, Phys. Rev. Lett. **106** 213901 (2011); A. Regensburger, C. Bersch, M.-A. Miri, G. Onishchukov, D.N. Christodoulides, and U. Peschel, Nature **488** 167 (2012)
- [5] N. Lazarides and G. P. Tsironis, Phys. Rev. Lett. **110** 053901 (2013)
- [6] I. L. Aleiner, B. L. Altshuler and Y. G. Rubo, Phys. Rev. B **85** 121301(R) (2012)
- [7] A. W. Snyder, J. D. Love, *Optical Waveguide Theory*. Chapman and Hall, London, 1983
- [8] C. Sparrow, *The Lorenz Equations: Bifurcations, Chaos, and Strange Attractors*. Appl. Math. Sci. **41** (1982) (Springer, New York)